On the accuracy assessment of a parallel robot for the minimally invasive cancer treatment

DOINA PISLA[1]*, BOGDAN GHERMAN [1], PAUL TUCAN [1], ADRIAN PISLA[1], NADIM AL HAJJAR[2], ANDREI CAILEAN[1], CALIN VAIDA[1]

[1]*Technical University of Cluj-Napoca, 28 Memorandumului, 400114 Cluj-Napoca, Romania*
[2]*"Iuliu Haţieganu" University of Medicine and Pharmacy, 8 Victor Babes, 400012 Cluj-Napoca, Romania*

Abstract. The paper focuses on the development of a robotic solution for cancer treatment. Liver cancer and especially hepatocellular carcinoma is one of the deadliest causes of death worldwide. Even more, liver cancer leads to more than half of the metastatic pancreatic cancers. Its treatment depends on the tumor staging and other comorbidities of the patient, and if the health condition is poor, minimally invasive procedures are preferred. The ProHep-LCT parallel robotic system has been developed for the minimally invasive treatment of cancer liver using various approaches: brachytherapy, radiofrequency ablation or intra-tumoral drug release, all of which requiring an accurate needle placement. ProHep-LCT has consists of two robots: one for tumor visualization using the intraoperative ultrasound technique and the other to deliver the targeted treatment. A research method regarding the onsite placement accuracy of the two modules of the ProHep-LCT using a commercial tracking system is proposed in the paper, to assess its usability for the medical task.

1. Introduction

With around 841,000 newly diagnosed cases and 782,000 fatalities per year, liver cancer ranks sixth among all cancers. The most frequent and deadliest form of liver cancer in the world is hepatocellular carcinoma (HCC), which is also the 5th most prevalent and deadliest type of cancer [1],[2]. Even though tumor excision is the optimal therapeutic approach (i.e. for patients with early diagnosis), only 20% of

---

*Correspondence address: doina.pisla@mep.utcluj.ro

HCC patients receive this treatment. Surgical resection is typically not advised for advanced stages of HCC since the patients are not strong enough to endure the procedure, [3]. Furthermore, minimally invasive surgical techniques can be used to accomplish 10–20% of all resections. Alternative approaches for treatment include radioembolization, trans arterial chemoembolization, and percutaneous local ablation, although these methods have poor accuracy [4]. The delivery of specialized chemotherapeutic drugs that only target malignant cells (intra-tumoral chemotherapy) and radiofrequency ablation (the treatment of a tumor by heating it to induce tumor necrosis) are three examples of targeted treatment for liver or pancreatic cancer that may be considered to reduce the cancer staging, which provides the opportunity for resection and organ transplant. The main advantages of these treatment methods include delivering the therapeutic agent in the desired place (reducing side effects as a result); and lowering the risk of trauma (such as piercing blood vessels that could result in hemorrhage).

Robotic devices are being employed more frequently in the medical profession, which has a positive social impact by raising the standard of living. Whether they are orthotic structures [5] or rehabilitation robots [6], [7], some of the most known and most popular are those in the field of human movement rehabilitation. The da Vinci system [8] is one of the most popular robotic systems for minimally invasive surgery (MIS), but there are other robotic systems for MIS that were developed, tested, and validated in clinical trials. On the other hand, various robotic structures have been designed and developed recently for surgical procedures, most notably for MIS [9] – [13]. Recent research has suggested the use of robotic systems for the targeted treatment of HCC with intra-tumoral chemotherapy or brachytherapy, [3]. In addition, the authors in [14] explored the potential for creating tailored treatment for HCC combining intra-tumoral chemotherapy and real-time image tracking (using US fused with CT). Intraoperative ultrasonography (I-US) coupled with preoperative CT is used in the suggested method to offer a safe and precise solution for inserting therapeutic needles within HCC under continuous imaging guidance.

Several methods have been proposed to assess the accuracy of medical robots. A quantitative method has been proposed in [15], where the CT has been used to assess the statistic accuracy of pedicle screws placement. In [16] the authors have used a 3D printed template to for the placement of brachytherapy needles and the accuracy has been evaluated using the CT intermediate set compared to the pre-implant CT dataset. The authors have assessed the usability of the OptiTrack motion system in [17] and [18], and proved that it is a stable and reliable system with an average error of 0.2 mm, which suits the accuracy requirements of the proposed medical task.

The current paper proposes a method to assess the accuracy of the ProHep-LCT parallel robotic system designed for needle placement procedures. Due to its proven performances, the Optritrack system has been used to measure the parallel robot end-effector position and orientation and thus assess the usability of the robotic system for the liver and pancreas cancers using needle placement medical approaches. The paper is organized as follows: section 2, Materials and methods,

presents the ProHep-LCT robotic system, mechanical and control architecture and the tracking equipment and proposed methodology used to assess the positioning accuracy in laboratory conditions; section 3, Results and discussions presents the obtained results and some explanations. The paper ends with section 4, Conclusions.

2. Materials and methods

2.1 The ProHep-LCT parallel robot

The proposed technical solution consists in a robotic system, ProHep - LCT, [14], [19], that is intended solve the three main problems that accuracy, patient safety, and procedural ergonomics present in brachytherapy and intra-tumoral treatment of HCC. ProHep-LCT kinematics, singularities and workspace analysis have been investigated [19], [20] in order to provide a proper operational workspace according to the operating field, patient safety and procedure ergonomics.

Fig. 1a presents the CAD model of the ProHep-LCT robotic system integrated into a virtual medical environment, with a patient positioned on the operating table. As previously mentioned, ProHep-LCT is a robotic system which consists of two robots sharing an identical architecture: the needle insertion robot, which guides the needle insertion robotic instrument and the intraoperative ultrasound (I-US) probe robot, which guides the I-US instrument, [21], [22]. Fig. 2b presents the experimental model of ProHep-LCT during initial experimental tests in laboratory environment.

Fig. 2 presents the mechanical architecture of the ProHep-LCT robot for needle insertion (identical with the I-US robot). The robot has 5 DoF which are used to guide the I-US and respectively the needle insertion robotic instruments. The robot consists of two parallel kinematic chains: the upper planar mechanism actuated by three active prismatic joints $\left(q_4 \text{ and } q_5\right)$ and the lower planar mechanism actuated by two revolute active joints $\left(q_2 \text{ and } q_3\right)$. The two planar mechanisms are connected via two universal joints $\left(U_1 \text{ and } U_2\right)$. Both planar mechanisms translate along the OZ axis using the prismatic joint q_1. The robot controls the end-effector coordinates $E\left(X_E, Y_E, Z_E\right)$ and its orientation, namely the angles $\psi \text{ and } \theta$, representing the rotation of the end-effector around the OY and OX axes. The mathematical model of the robot has been detailed in [10].
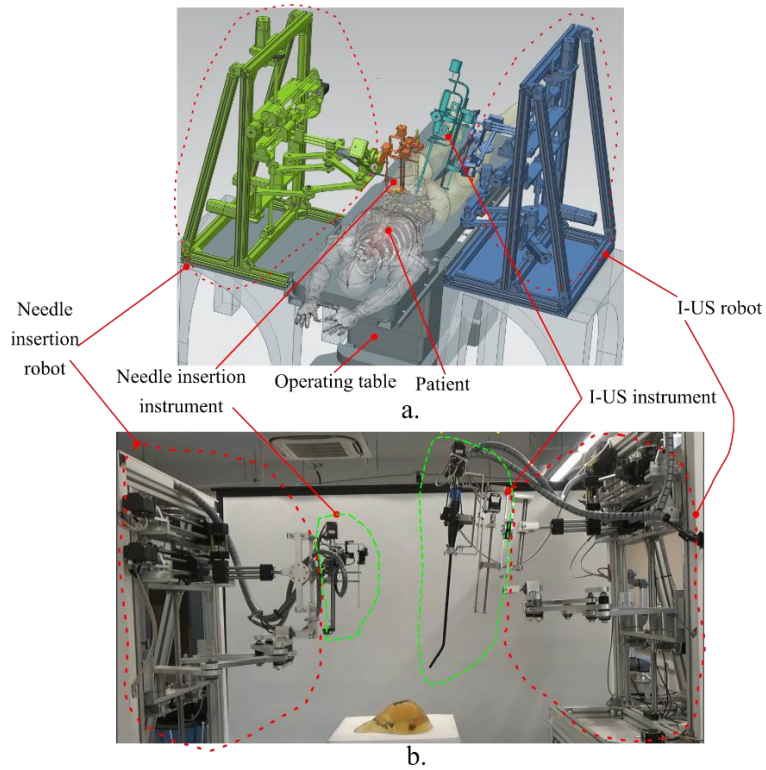
Fig. 1. The ProHep-LCT robotic system: a. the CAD model in virtual medical environment;
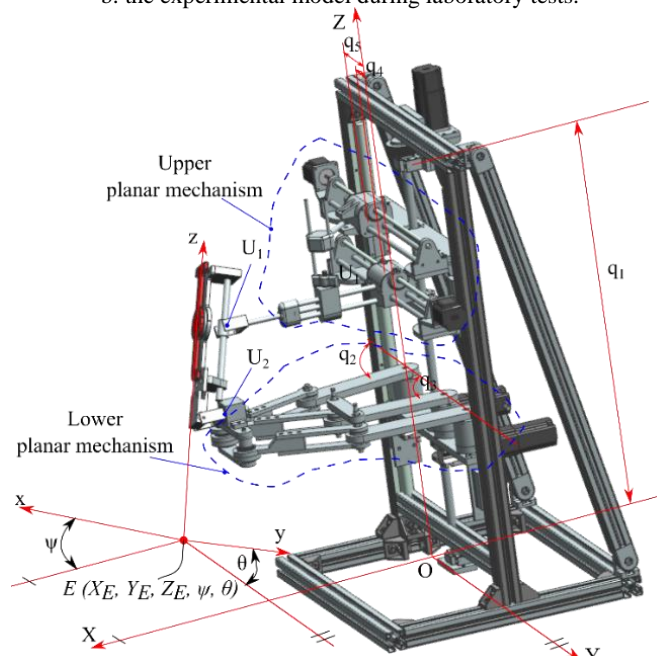b. the experimental model during laboratory tests.

Fig. 2. The ProHep-LCT robot for needle insertion.

The I-US instrument (Fig. 3a) has 4 degrees of freedom (DoF) used to insert the I-US probe (which is a Hitachi Arietta 70, [14]) on a linear trajectory, rotate the I-US probe and actuate the two levers which guide the transducer. The I-US helps the surgeon read the position of the target points in the tumor which are further sent to the needle insertion robot in charge of placing the needles. ProHep-LCT has been designed to insert straight needles on a linear trajectory in a minimal invasive approach, meaning that the needles are inserted percutaneously (from the outside of the patient's body). For this task, the needle insertion robot positions the needle insertion instrument (Fig. 2b) in the vicinity of the insertion point from where the needle insertion module continues the insertion procedure. It is a 3+1 DoF mechanism using a Gantry architecture which positions the needles at the insertion point in the OXY plane and performs the needle insertion (along the OZ axis). The last motor is used to actuate the gripper. The needle insertion instrument has been designed to insert up to 6 brachytherapy needles, which are stored in the needle rack. Each needle to be inserted is gripped and removed from the needles rack, positioned above the insertion point and inserted following the linear trajectory.
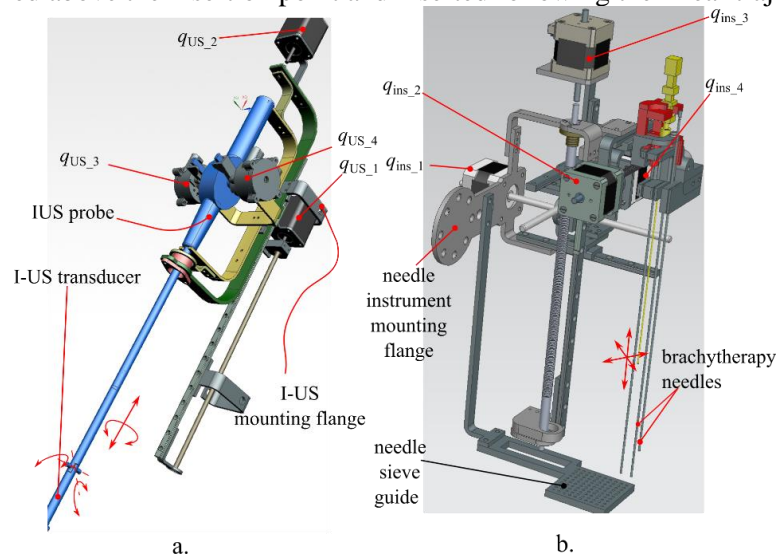

Fig. 3.The ProHep-LCT robotic instruments: a. the I-US guiding instrument;
b. the needle insertion instrument.

2.2 The ProHep-LCT control architecture

The ProHep-LCT control strategy uses a Continuous Path Motion strategy implemented within the control system. It can move from point P_1 to point P_2 following a linear trajectory discretized into several steps computed using a time increment, to strictly control the motion parameters along the followed path. The end effector position and orientation, and the motion parameters are through integration, based on the maximum velocity and acceleration of the end-effector and an imposed trapezoidal motion profile for the velocity. Using the inverse

kinematics, the active joints position, velocity and acceleration is further computed. Fig. 4 presents the motion control strategy of the ProHep-LCT robotic system.
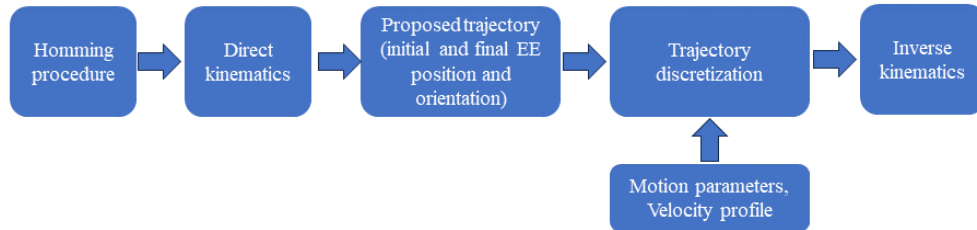

Fig. 4. The ProHep-LCT control system – physical model.

Fig. 4 presents the control architecture of the ProHep-LCT robotic system. The selected control components are from B&R Automation Gmbh, company specialized in the development of motion control equipment, [23]. The User interface has been detailed in [22]. ProHep-LCT system is controlled using a PLC (model X20CP3586), dual axes driver ACOPOSmicro modules (80sd100xd.c044-01), with the stepper motors within the NEMA 23 – NEMA 11 range with encoders, according to the specific task and inductive proximity sensors to perform the initialization procedure.
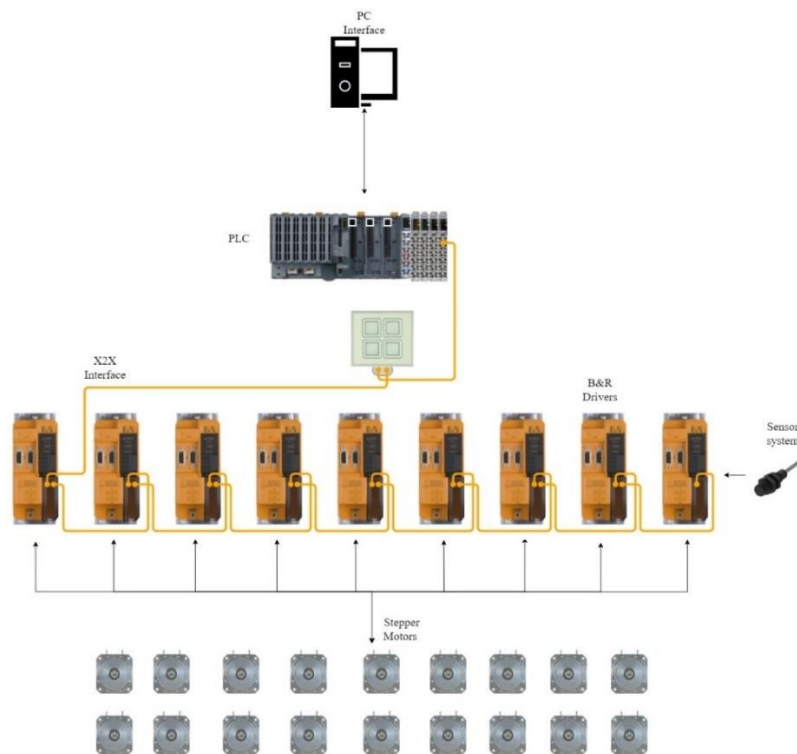

Fig. 5. The ProHep-LCT control system – physical model.

2.3 Accuracy assessment methodology

The ProHep-LCT robotic system accuracy has been assessed in laboratory conditions using the OptiTrack Motion Capture System, [7]. OptiTrack was originally developed to capture human (and rigid) body motions using a set of predefined markers accurately positioned on the tracking objects. In this case the markers M3 with a 6.4 mm diameter (with M3 Marker Base) and have been placed on the mechanical structure. Fig. 6 presents the marker's placement on the mobile platform (where the robotic instruments are attached) and on the robot frame, to be used for a correct definition of the reference frame. In addition, the calibration of the OptiTrack system requires the CS-400 calibration square (Fig. 7), which has been further used to correctly set the OXYZ coordinate system. A set of six Prime 41 infrared cameras with 170 LEDs have been used within the current setup (the number of cameras can vary according to the monitored workspace). The markers have been accurately placed following a calibration procedure consisting in 4 steps (for the end-effector):

1. Bring the robot into the Origin position. The Origin position considers the end-effector (mobile platform) orientation as: $\psi = 0$ and $\theta = 0$.

2. Position as accurately as possible the two markers on the end-effector.

3. Perform an initial set of measurements using OptiTrack and check that the two angles fit the proposed orientation. Check that the end-effector tip (the lower marker in Fig. 6) fits the input values fed into the control system.

4. If the measured values fit the mathematical model, the calibration is successful, otherwise the marker's position needs to be re-adjusted according to the measurements.
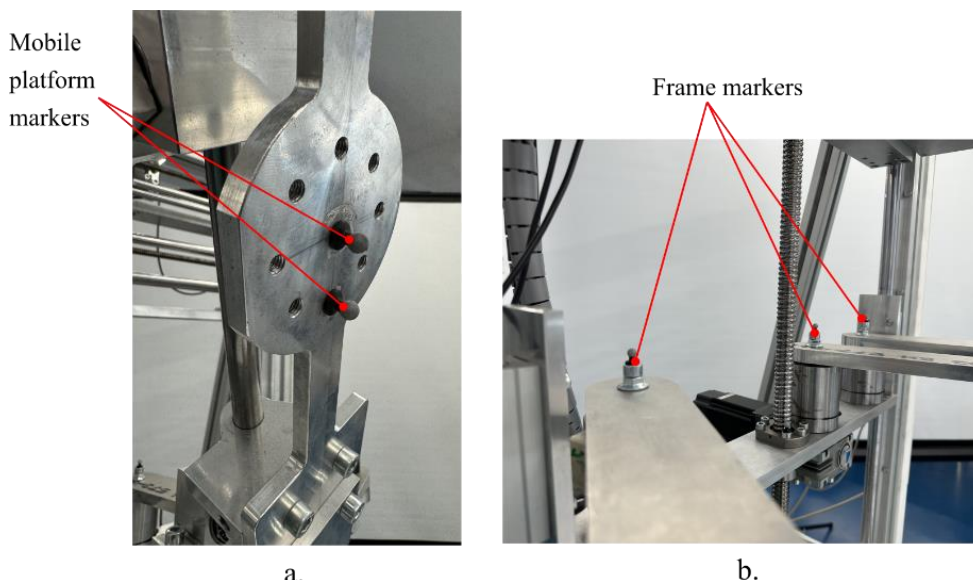
Fig. 6. Markers mounted on the ProHep-LCT.

The robot end-effector coordinates $E\left(X_E, Y_E, Z_E\right)$ are provided directly by the Motive software [17] which is used to process the OptiTrack data provided by the cameras, after the translation of the OXYZ coordinate system into the position indicated in Fig. 7, which represents the OptiTrack perspective view of the markers.

The markers labeling has been performed automatically, which resulted in the number presented in Fig. 8. The end-effector orientation has been determined as follows:

1. Determine the equations of the two planes XOZ and YOZ using the markers position provided by the Motive:

$$A_{XOZ} \cdot x + B_{XOZ} \cdot y + C_{XOZ} \cdot z + D_{XOZ} = 0 \tag{1}$$

$$A_{YOZ} \cdot x + B_{YOZ} \cdot y + C_{YOZ} \cdot z + D_{YOZ} = 0 \tag{2}$$

2. Determine the equation of the end-effector markers line (auto-labeled as 1126 and 1127 in Fig. 7):

$$l = \left(x_{M1} - x_{M2}\right); m = \left(y_{M1} - y_{M2}\right); n = \left(z_{M1} - z_{M2}\right) \tag{3}$$

Yielding:

$$\frac{x - x_{M2}}{l} = \frac{y - y_{M2}}{m} = \frac{z - z_{M2}}{n} \tag{4}$$

3. Determine the angles:

$$\sin\left(\theta\right) = \frac{\left|A_{XOZ} \cdot l + B_{XOZ} \cdot m + C_{XOZ} \cdot n\right|}{\sqrt{A_{XOZ}^2 + B_{XOZ}^2 + C_{XOZ}^2} \cdot \sqrt{l^2 + m^2 + n^2}} \tag{5}$$

$$\sin\left(\psi\right) = \frac{\left|A_{YOZ} \cdot l + B_{YOZ} \cdot m + C_{YOZ} \cdot n\right|}{\sqrt{A_{YOZ}^2 + B_{YOZ}^2 + C_{YOZ}^2} \cdot \sqrt{l^2 + m^2 + n^2}} \tag{6}$$
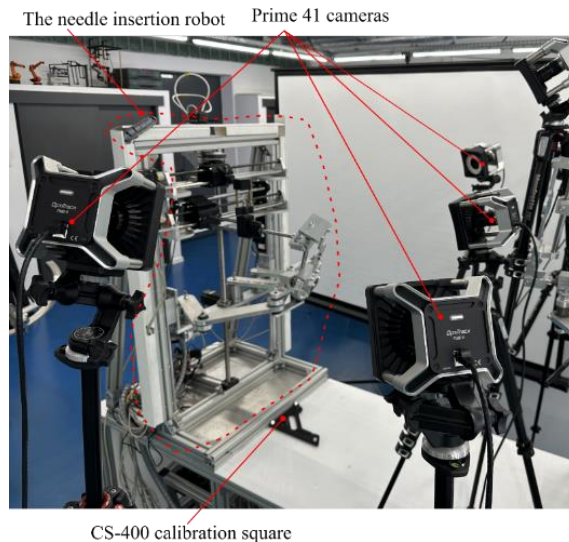

Fig. 7. The ProHep-LCT robotic system with the OptiTrack motion tracking system.
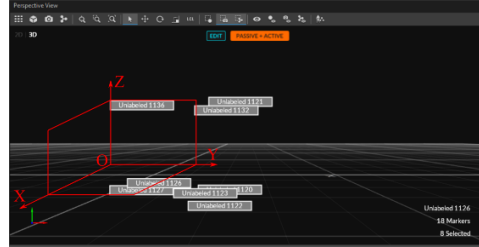
Fig. 8. The ProHep-LCT parallel robot with the OptiTrack motion tracking system.

3. Results and discussions

To assess the accuracy of the ProHep-LCT robotic system, the following trajectory of the end-effector has been proposed:

$$X_{E\_init} = 560mm; Y_{E\_init} = 490mm; Z_{E\_init} = 230mm; \psi_{init} = 40^o; \theta_{init} = 20^o \qquad (7)$$

$$X_{E\_fin} = 600mm; Y_{E\_fin} = 530mm; Z_{E\_fin} = 200mm; \psi_{fin} = -34^o; \theta_{fin} = 27.2^o \qquad (8)$$

Figures 9 – 13 present the results of the measurement using the OptiTrack system, after applying a Fast Fourier Transform (FFT) to denoise the measured signal.
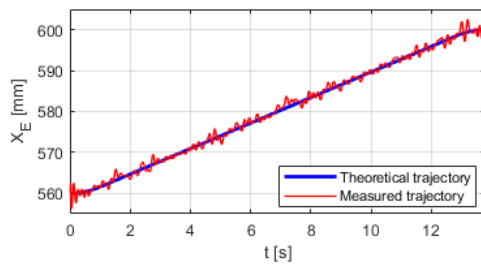

Fig. 9. The ProHep-LCT needle insertion robot comparative time history diagram for the X coordinate of the end-effector.
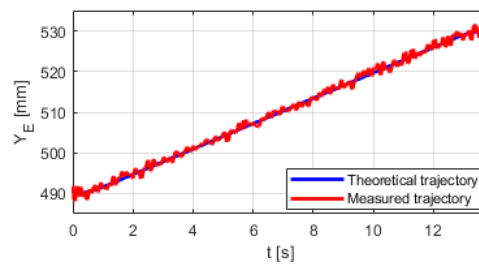

Fig. 10. The ProHep-LCT needle insertion robot comparative time history diagram for the Y coordinate of the end-effector.
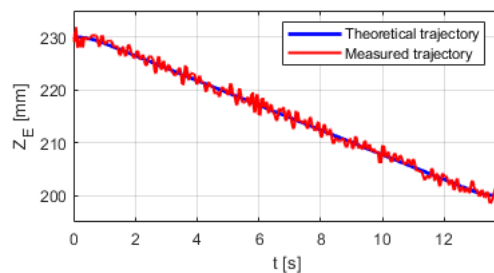

Fig. 11. The ProHep-LCT needle insertion robot comparative time history diagram for the Z coordinate of the end-effector.
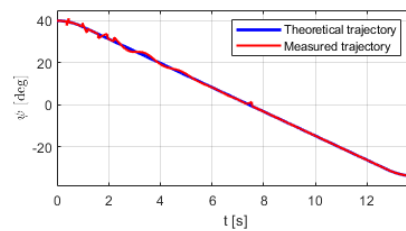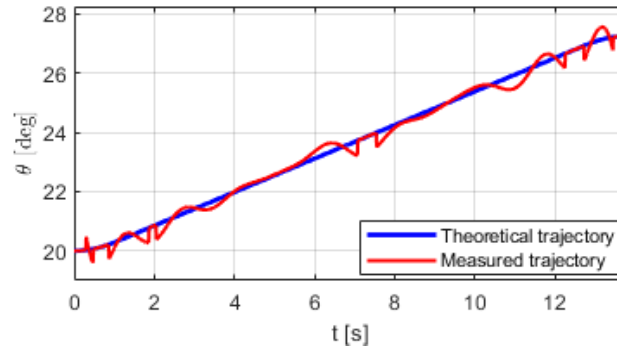

Fig. 12. The ProHep-LCT needle insertion robot comparative time history diagram for the ψ coordinate of the end-effector.

Fig. 13 The ProHep-LCT needle insertion robot comparative. time history diagram for the θ
coordinate of the end-effector.

Five measurements have been performed and the Mean Root Mean Square Error is presented in Table 1. The data show a good correlation between the theoretical modeled trajectory and the measured one. The mean positioning accuracy of the end-effector is 0.883 mm, which can be considered as good for the first iteration of the experimental model. The required accuracy for the needle placement in brachytherapy procedures is of 1 mm [10] in the air. The most problematic issue consists of needle deflection, which is very probable and difficult to control. Nevertheless, within certain limits, the needle placement errors caused by the needle deflection can be adjusted by using stronger radioactive seeds and keep them for a longer period within the tumor.

The main sources of error are the OptiTrack's own accuracy, the light sources within the room, which negatively impacts markers tracking, the trapezoidal screws and revolute joints play (the backlash of the worm gears have not introduced errors for the proposed trajectory).

Table 1. Root Mean Square Error for the measured data using OptiTrack

End-effector coordinate	Root Mean Square Error
X_E	0.6781
Y_E	0.7482
Z_E	0.5614
ψ	0.4754
θ	0.4229

4. Conclusions

The paper presents the accuracy assessment in laboratory conditions of the ProHep-LCT robotic system. The OptiTrack motion tracking system has been used to perform a set of measurements of the ProHep-LCT needle insertion robot, mechanically identical to the I-US robot. The comparative results show that ProHep-LCT has good accuracy, both regarding the coordinates of the end-effector

and its orientation. Future work will focus on the real-time implementation of a supervising mechanism using OptiTrack within the control system of ProHep-LCT, which should adjust the final pose of the end-effector.

Acknowledgements

References

[1]   Chen S., Cao Q., Wen W., Wang H., *Targeted therapy for hepatocellular carcinoma: Challenges and opportunities,* Cancer Lett, **460**, 2019, p. 1-9.

[2]   Vaida C., Al Hajjar N., Lazar V., Graur F., Burz A., Elisei R., Mois E., Pisla D., *Robotics in minimally invasive procedures: History, current trends and future challenges*, the 6th Int. Conf. on Advancements of Medicine and Health Care through Technology – MediTech 2018, 17-20 October 2018, p. 267-273.

[3]   Pisla D., Calin V., Birlescu I., Hajjar N.A., Gherman B., Radu C., Plitea N., *Risk Management for the Reliability of Robotic Assisted Treatment of Non-resectable Liver Tumors*, Appl. Sci. 2020, **10**, 52, 2020.

[4]   Yang Z., He W., Zheng Y., Zou R., Liu W., Zhang Y., Wang C., Wang Y., Yuan Y., Li B., Yuan Y., *The efficacy and safety of long-versus short-interval transarterial chemoembolization in unresectable hepatocellular carcinoma*, Journal of Cancer, **9**, 21, 2018, p. 4000-4008.

[5]   Pisla D., Tarnita D., Tucan P., Tohanean N., Vaida C., Geonea I.D., Gherman B., Abrudan C., Carbone G., Plitea N., *A Parallel Robot with Torque Monitoring for Brachial Monoparesis Rehabilitation Tasks*, Appl. Sci., **11**, 2021, 9932.

[6]   Vaida C., Birlescu I., Pisla A., Ulinici I.M., Carbone G., Pisla D., *Systematic Design of a Parallel Robotic System for Lower Limb Rehabilitation*, IEEE Access, **8**, 2020, p. 307-322.

[7]   Gherman B., Birlescu I., Nicolae P., Carbone G., Tarnita D., Pisla D., *On the singularity-free workspace of a parallel robot for lower-limb rehabilitation*, Proc. Rom. Acad. Series A, **20**, 4, 2019, p. 383-391.

[8]   van der Schans E.M., Hiep M.A.J., Consten E.C.J., Broeders I.A., *From Da Vinci Si to Da Vinci Xi: realistic times in draping and docking the robot*, J Robotic Surg, **14**, 2020, p. 835–839.

[9]   Pisla D., Gherman B., Plitea N. et al., *PARASURG hybrid parallel robot for minimally invasive surgery*, Chirurgia, **106**, 5, p. 619-625, 2011.

[10]   Vaida C., Plitea N., Al Hajjar N., Burz A., Graur F., Gherman B., Pisla D., *A new robotic system for minimally invasive treatment of liver tumours*, Proc. Rom. Acad. Series A, **21**, 3, 2020, p. 263-271.

[11]   Vaida C., Pisla D., Schadlbauer J., Husty M., Plitea N., *Kinematic Analysis of an Innovative Medical Parallel Robot Using Study Parameters*, Wenger, P., Chevallereau, C., Pisla, D., Bleuler, H., Rodić, A. (eds) *New Trends in Medical and Service Robots*, Mechanisms and Machine Science, **39**, Springer, Cham. 2016, p. 85-99.

[12]   Pisla D., Plitea N., Vidrean A., Prodan B., Gherman B., Lese D., *Kinematics and Design of two variants of a reconfigurable parallel robot*, Proceedings of the 2009 ASME/IFToMM International Conference on Reconfigurable Mechanisms and Robots, London, UK, 22–24 June 2009; p. 624–631.

[13]   Brett P. N., Taylor R. P., Proops D., Coulson C., Reid A., Griffiths M. V., *A surgical robot for cochleostomy*, Proceedings of the 29th Annual International Conference of the IEEE Engineering in Medicine and Biology Society (EMBS), Lyon, France, 2007, p. 1229–1232.

[14]   Radu C, Fisher P, Mitrea D, Birlescu I, Marita T, Vancea F, Florian V, Tefas C, Badea R, Ştefănescu H, Nedevschi S., Pisla D., Al Hajjar N., *Integration of Real-Time Image Fusion in the Robotic-Assisted Treatment of Hepatocellular Carcinoma*, Biology, **9**, 11, 2020, p. 397.

[15]   Benech C.A., Perez R., Benech F., Shirk T., Bucklen B.S., *A quantitative accuracy assessment of the use of a rigid robotic arm in navigated placement of 726 pedicle screws*, BMC Surg, **22**, 385, 2022.

[16]   Huang M.W., Zhang J.G., Zheng L., Liu S.M., Yu G.Y., *Accuracy evaluation of a 3D-printed individual template for needle guidance in head and neck brachytherapy*, J Radiat Res., **57**, 6, 2016 Nov, p. 662-667.

[17]   Chen Q., Zhou Y., Wang Y., Zhu M. M., Guo L., He C. X., *Research on stability and accuracy of the OptiTrack system based on mean error*, International Symposium on Artificial Intelligence and Robotics, 11884, 2021.

[18]   Ameler T. et al., *A Comparative Evaluation of SteamVR Tracking and the OptiTrack System for Medical Device Tracking*, 2019 41st Annual International Conference of the IEEE Engineering in Medicine and Biology Society (EMBC), Berlin, Germany, 2019, p. 1465-1470

[19]   Vaida C., Plitea N., Al Hajjar N., Burz A., Graur F., Gherman B., Pisla D., *A New Robotic System For Minimally Invasive Treatment of Liver Tumours*, Proc. Rou. Acad., Series A, **21**, 3, 2020, p. 263-271.

[20]   Birlescu I., Husty M., Vaida C., Pisla D., *Complete Geometric Analysis Using the Study SE (3) Parameters for a Novel, Minimally Invasive Robot Used in Liver Cancer Treatment*, Symmetry, **11**, 2019, p. 1491.

[21]   Gherman B., Al Hajjar N., Burz A., Birlescu I., Tucan P., Graur F., Pisla D., *Design of An Innovative Medical Robotic Instrument for Minimally Invasive Treatment of Liver Tumors*, Acta Technica Napocensis, **64**, 4, 2019, p. 557-562.

[22]   Gherman B., Birlescu I., Burz A., Ulinici I., Tucan P., Pisla D., *Kinematic Analysis of Two Innovative Medical Instruments for the Robotic Assisted Treatment of Non-resectable Liver Tumors*, EuCoMeS 2020, Mechanisms and Machine Science, **89**, Springer, Cham., 2020, p. 189-197.

[23]   https://www.br-automation.com/en/products/plc-systems/x20-system/x20-plc/x20cp3586/, last accessed 2023/07/11.